Electron Sputtering in the Analytical Electron Microscope: Calculations and Experimental Data

by Nestor J. Zaluzec and John F. Mansfield, Electron Microscopy Center for Materials Research, Materials Science & Technology Division, Argonne National Laboratory, Argonne, Illinois 60439 U.S.A.

Introduction

The environment of the electron microscope is particularly severe when one considers the energy deposited in a specimen during typical experimental conditions. Conventional imaging experiments tend to employ electron current densities ranging from ~ 0.1 to 1 A/cm^2, while during microanalysis conditions probe current densities can range from 10 to values as high as 10^5 A/cm^2. At 100 kV this corresponds to power densities from 100 Kilowatts/cm^2 to 10^4 Megawatts/cm^2. We have long known that these energy deposition rates can result in electron irradiation damage which can substantially alter the structure and composition of a specimen through either ionization damage in organics (Glaeser, 1978) or by displacement damage in inorganics (Hobbs, 1978) and/or combinations thereof. For the most part materials scientists operating an analytical electron microscope (AEM) in the 100–200 kV regime studying metallic and/or ceramic specimens have been spared the need to consider either of these effects as their specimens have tended to be sufficiently resilient. However, the advent of the new medium voltage microscopes operating in the 300–400 kV regime with high brightness guns and clean or ultrahigh vacuum systems has necessitated a reevaluation of the effects of higher voltage operation in light of the destructive nature of the electron beam particularly under microanalysis conditions.

The advantages of increasing the accelerating voltage and decreasing the column vacuum have been discussed in detail elsewhere (Zaluzec 1978, Zaluzec, Taylor, Ryan & Philippides 1983, as well as in these proceedings).* The detrimental implications of higher voltage operation relative to microanalysis are more subtle and were briefly discussed by Zaluzec and Mansfield (1986). In this earlier work, the calculated rates of displacement damage and atomic sputtering were compared with the characteristic signal generation rate. In this paper we expand upon that study with additional calculations relative to atomic sputtering as well as provide experimental verification of electron beam induced sputtering in the AEM.

Radiation Damage and Sputtering

Radiation displacement damage occurs when kinetic energy is transferred from the incident electron beam to the atoms within the specimen. If the energy transferred is sufficient, then atoms may be displaced from their lattice sites, either to form point defects, which may subsequently migrate and cause elemental rearrangement, or to be sputtered from the solid. These effects have been widely reported in the literature over the last ten years, however they have been mainly associated with High Voltage Electron Microscope (HVEM) studies (see for example Wiedersich et al 1977; Cherns et al 1976, 1977; Okamoto and Lam 1985). More recently electron probe related effects have been observed at 100 kV in dedicated STEM instruments by Mochel et al (1983) and Thomas (1985) while radiation induced segregation was also observed by Mansfield et al (1986) during X-ray Energy Dispersive Spectroscopy (XEDS) analysis of an aluminium zinc alloy at 300 kV.

The amount of kinetic energy (T_T) transferred by an incoming electron (mass m_o) to the nucleus of a specimen atom depends upon its kinetic energy $T_E = eV_o$ (e = electronic charge, V_o = accelerating potential), the mass of the nucleus (M) and the direction of scattering (ϕ) and can be written:

$$T_T = [2*T_E*(T_E + 2*m_oc^2)*\sin^2(\phi/2)]/[Mc^2] \quad (1)$$

The maximum energy transfer occurs for the forward scattering geometry ($\phi = 180°$), which is the condition that we will use in all the calculations presented herein. Atomic displacement occurs when the incident electron transfers sufficient energy (T_d) to permanently displace or remove an atom from its normal lattice site. For the case of sputtering in the AEM, we consider only the removal of atoms from the electron exit surface of the specimen. Since the atoms at this surface are not totally surrounded as in the "bulk", the sputtering energy required to remove them (T_s) is necessarily less than that required to form defects within the solid. As an upper limit one can estimate that $T_s \sim T_d/2$. Phenomenologically, T_s can also be related to the sublimination energy of a material; this could lower estimates of T_s by as much as another factor of 2. Table 1 compares the maximum kinetic energy transferable to various atoms at accelerating voltages of 100–400 kV, with values of the experimentally derived displacement energy T_d and the sputtering energy $T_d/4 < T_s < T_d/2$. As one can see from this table the amount of energy transferred (T_T) to many elements in the 100–400 kV range is equal to or greater than T_s and therefore sufficient to warrant further investigation particularly for elements of atomic number < 30.

Table 1
Comparison of Maximum Transferable Kinetic Energy with Displacement and Sputtering Energies at 100, 200, 300 and 400 kV

Element	T_T[eV]				T_d[eV]	T_s[eV]
	100 kV	200 kV	300 kV	400 kV		
Al	8.93	19.5	31.6	45.3	16	4–8
Ti	5.00	11.0	17.8	25.5	15	4–8
V	4.73	10.3	16.72	24.0	29	7–14
Cr	4.63	10.1	16.38	23.5	22	5–11
Fe	4.31	9.40	15.25	21.8	16	4–8
Co	4.08	8.91	14.45	20.7	23	6–12
Ni	4.10	8.94	14.5	20.8	22	6–11
Cu	3.79	8.26	13.4	19.2	18	4–9
Zn	3.69	8.03	13.03	18.7	16	4–8
Nb	2.59	5.65	9.17	13.2	24	6–12
Mo	2.51	5.47	8.88	12.7	27	7–14
Ag	2.23	4.87	7.90	11.3	28	7–14
Cd	2.14	4.67	7.58	10.9	20	5–10
Ta	1.33	2.90	4.71	6.75	33	8–16
Pt	1.23	2.69	4.37	6.26	33	8–16
Au	1.22	2.67	4.32	6.2	36	9–18

In order to estimate the cross sections (σ) for sputtering, we will assume values of $T_s \sim T_d/2$ and then interpolate values of σ from Oen's tables (1973). Sputtering cross sections obtained in this manner are plotted in Figure 1 for the elements aluminium, titanium, nickel and niobium. The sputtering rate (R_s) is given by the product of the cross-section (σ) and the probe current density (J). Although the cross-sections shown in Figure 1 are somewhat low (1–100 Barns) the probe current density found under microanalysis conditions can be sufficient to make the sputtering rates significant. For example, one calculates that at 400 kV for a probe current density of 30 A/cm^2 the sputtering rates for aluminium, titanium, nickel and niobium are 0.020, 0.025, 0.011, and 0.002 displacements/atom/sec, respectively. Assuming that each displacement of a

*National Research Council, Ottawa, Canada Intermediate Voltage Conference (See note in Table of Contents)

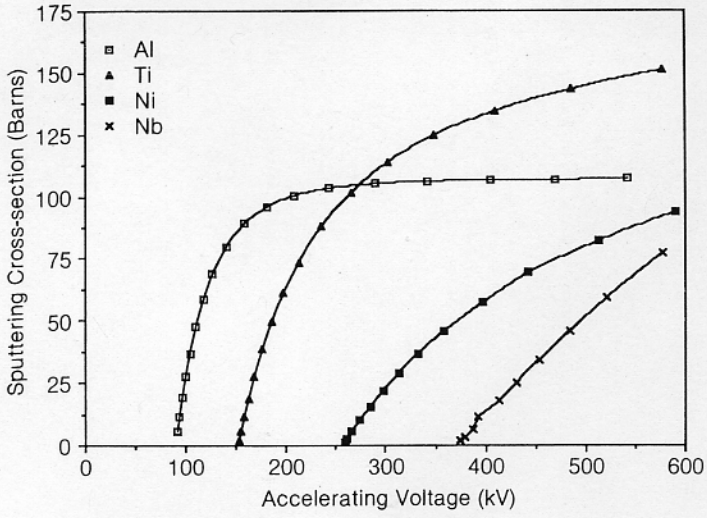

Figure 1. Sputtering cross-sections for aluminium, titanium, nickel and niobium as a function of the incident beam accelerating voltage evaluated for $T_s = T_d/2$.

surface atom is sufficient to cause its removal then the magnitude of this displacement or sputtering rate (~0.02–0.002 atomic layers per second) should be readily observable. With the advent of the high brightness LaB_6 and Field Emission Guns having current densities as much as 10 to 1000 times greater, one clearly has the potential to encounter enormous sputtering rates during microanalysis. This, of course, assumes that the environmental conditions within the microscope at the specimen are sufficiently "clean" that hydrocarbon contamination in the vicinity of the probe does not overwhelm the process of surface sputtering.

Experimental

A thin foil of a polycrystalline aluminium-magnesium alloy was prepared by co-evaporation in a UHV evaporation system on NaCl. After removal of the NaCl by clean distilled water the specimen was mounted upon 3 mm copper grid and subsequently transferred to the AEM. The specimen was irradiated with a 180 nm diameter probe in a Philips EM420T for approximately 4000 seconds at 120kV using a tungsten hairpin filament electron source. The electron probe current was measured with a post-specimen Faraday cup, located in the

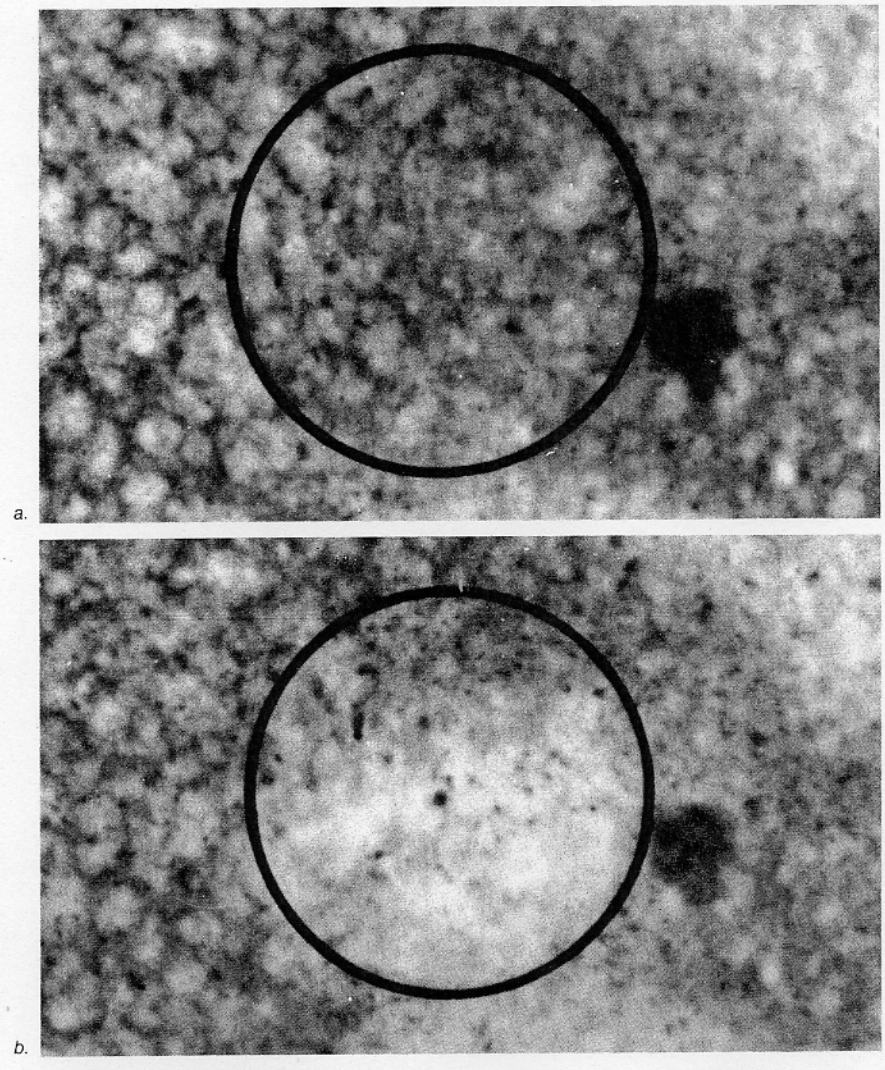

Figure 2. Analyzed region of the aluminium/magnesium alloy before (a) and after (b) 4000 sec irradiation. Thinning due to sputtering is readily visible in the micrograph.

camera chamber of microscope, where it was determined that during the sputtering experiment the probe current density was constant at ~ 28 A/cm^2. Figure 2 shows a micrograph of the irradiated area before (2a) and after (2b) the 4000 sec irradiation, clearly seen is the "thinning" of the selected area. No specimen contamination during microanalysis of this specimen was observed at any time during this study in the AEM.

The change in relative thickness of the sample was monitored by continuously measuring the low loss region of the electron energy loss spectrum of the irradiated area and using the expression:

$$T/\lambda = 1n(I_o/I_t) \qquad (2)$$

where T = specimen thickness, λ = mean free path of the inelastically scattered electrons, I_o = intensity of the zero loss peak, and I_t = intensity of the total inelastic spectrum. The values of $1n(I_o/I_t)$ were plotted as a function of irradiation time and the resulting graph is shown in Figure 3. This plot illustrates that there was a continuous reduction in the sample thickness during the irradiation which we attribute to sputtering.

A semi-quantitive analysis of the change in thickness can be made by assuming that the value of λ for the alloy is nearly the same as that for pure aluminium (~120 nm). Thus assuming that the thickness calculated from the time zero spectrum is the original thickness, then this data yields an initial thickness of 62.4 nm and a final thickness of 42.0 nm. This represents a ~20 nm (33%) reduction in sample thickness in the area under the probe due to the irradiation.

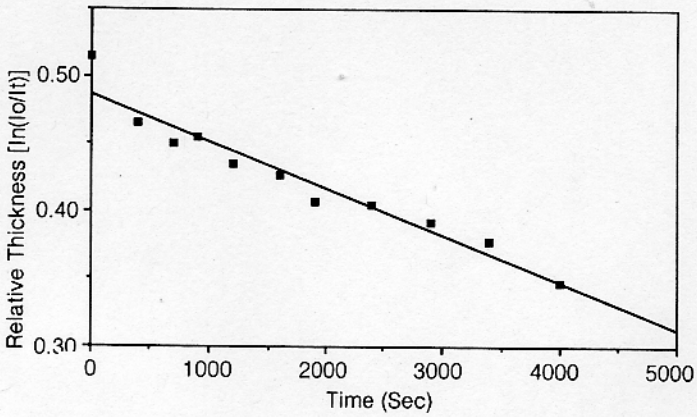

Figure 3. Experimentally measured change in specimen thickness during irradiation, obtained by continuously measuring the relative intensity of the zero loss to inelastic scattering intensity ratio during electron irradiation.

For comparison, the reduction in thickness by sputtering can be also estimated using calculated sputtering rates discussed above. Cross-sections for sputtering at 120 kV were interpolated from Oen's calculations for pure aluminium and magnesium. The interpolation for pure Al is relatively unambiguous and yields a value of ~62 barns. Magnesium, however, is more difficult as the data is rapidly varying in the region in which we are interested; here the cross section is estimated to lie between 75 and 150 barns. For an irradiation time of 4000 seconds, with a probe current density of 28 A/cm^2, the amount of each element sputtered would have been ~43 layers of Al and ~52–104 layers of Mg. If we assume for the purposes of comparison that each atomic layer is ~0.3 nm thick equally populated by Al and Mg, then one calculates an overall reduction in thickness of ~15–28 nm which compares favorably to the experimentally determined mass loss of 20 nm.

The loss of mass, during microanalysis, from a specimen would, on purely statistical considerations, merely require an extended acquisition time in most microanalysis situations. However, examination of XEDS spectra recorded both at the beginning and the end of the irradiation (Figure 4) revealed that there was also preferential removal of magnesium. Thus, the sample composition was changing during the irradiation, an effect which is to be expected considering the fact that the atomic sputtering rates for the two species are different.

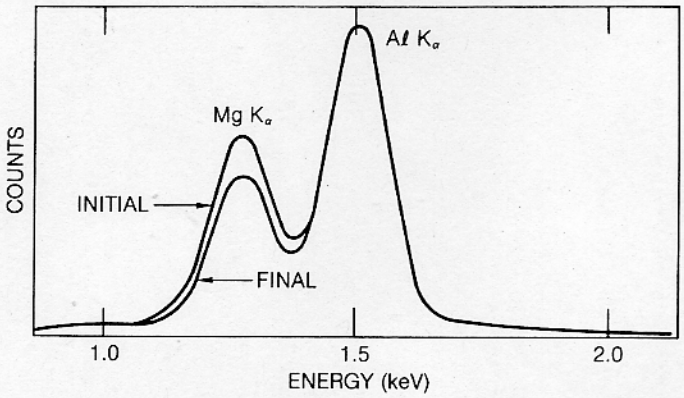

Figure 4. Experimentally measured X-ray energy dispersive spectra before and after ~4000 sec irradiation. Note the change in the relative intensity ratio of Al to MgKα lines indicating a preferential loss of Mg due to sputtering. The Al Kα lines have been normalized to the same value for display purposes.

Conclusions

Experimental measurement of the atomic sputtering of specimens during microanalysis in a conventional 120 kV AEM, has verified that electron sputtering can be an important effect during microanalysis. Calculations indicate that for the new generation of medium voltage analytical electron microscope this effect will become even more pronounced and must not be neglected during analysis. Preferential sputtering of different atomic species was observed and can have major implications to the accuracy of quantitative microanalysis.

Acknowledgement

This work was supported by the U.S. Department of Energy, BES Materials Sciences, under contract number W-31-109-ENG-38 at Argonne National Laboratory.

References

Cherns, D., Minter, F. J. and Nelson, R. S., (1976) Nucl. Inst. & Methods *132*, 369.

Cherns, D., Finnis, M. W. and Matthews, M. D., (1977) Phil. Mag. *35*, 693.

Glaeser, R. M., in Introduction to Analytical Electron Microscopy, ed. Hren, Joy, and Goldstein (1978) Chapter 16, Plenum Press.

Hobbs, L. W. in Introduction to Analytical Electron Microscopy, ed. Hren, Joy, and Goldstein (1978) Chapter 17 Plenum Press.

Mansfield, J. F., Okamoto, P. R., Rehn, L. E. and Zaluzec, N. J., accepted for publication in Ultramicroscopy 1986.

Mochel, M. E., Humphreys, C. J., Eades, J. A., Mochel, J. M. and Petford, A. M., (1983) Applied Physics Letters, Vol 42 (4), *392*.

Oen, O. S., (1973) ORNL Report #TM-4897.

Thomas, L. E., (1985) Ultramicroscopy *18*.

Wiedersich, H., Okamoto, P. R., Lam, N. Q. (1977) in Radiation Effects in Breeder Reactor Structural Materials, ed. M. L. Bleiberg and J. W. Bennett (AIME, New York) 801–809.

Zaluzec, N. J. (1978) 9th Int. Cong. on E. M., Toronto, Canada, 548.

Zaluzec, N. J., Taylor, A., Ryan, E. A. and Philippides, A., (1983) Proc 7th HVEM Meeting, Univ. of Calif., Berkeley, Ca., #LBL-16031 Conf.-830819 79.

Zaluzec, N. J., Mansfield, J. F., Okamoto, P. R. and Lam, N. Q., (1985) Inst. Phys. Conf. Series No. 78.

Zaluzec, N. J. and Mansfield, J. F., (1986) Proceedings of the 44th EMSA meeting Albuquerque N.M., 708, San Francisco Press ed. G. W. Bailey.